Chinese Chemical Letters 31 (2020) 715–720

Contents lists available at ScienceDirect

Chinese Chemical Letters

journal homepage: www.elsevier.com/locate/cclet

Communication

Aerosol-assisted submicron γ-Fe_2O_3/C spheres as a promising heterogeneous Fenton-like catalyst for soil and groundwater remediation: Transport, adsorption and catalytic ability

Jingjing Zhan[a,*], Mingfei Li[a], Xiujuan Zhang[b], Yu An[a], Weiqi Sun[a], Aixia Peng[a], Hao Zhou[a]

[a] School of Food and Environment, Dalian University of Technology, Panjin 124221, China
[b] School of Petroleum and Chemical Engineering, Dalian University of Technology, Panjin 124221, China

ARTICLE INFO

Article history:
Received 23 July 2019
Received in revised form 22 August 2019
Accepted 2 September 2019
Available online 4 September 2019

Keywords:
Heterogeneous Fenton
Groundwater remediation
Aerosol-assisted materials
Transport
Adsorption

ABSTRACT

This research reports a novel heterogeneous Fenton-like catalyst which could freely move through the model sediments and easily seize the pollutants in addition to efficiently catalyze H_2O_2, well suitable for soil and groundwater remediation. Herein, submicron γ-Fe_2O_3/C spheres were synthesized through a facile one-step aerosol-based process. In a series of column tests, these spheres exhibit better transport ability due to their optimal size, conforming to the prediction by the Tufenkji–Elimelech filtration theory. Meanwhile, γ-Fe_2O_3/C spheres could act as a strong adsorbent for organic pollutants owing to the presence of carbon, thereby providing a driving force to gather contaminants into their vicinity and facilitating the reaction. In addition, immobilization of γ-Fe_2O_3 nanoparticles into carbon spheres protects iron oxides from aggregation, and thus retains the number of active sites for catalytic decomposition of H_2O_2. Hence, the system containing the as-prepared γ-Fe_2O_3/C spheres and H_2O_2 shows the high removal efficiency and degradation efficiency in the remediation of recalcitrant organic contaminants such as methylene blue and sulfamethoxazole.

With the rapid growth of population, environmental pollution has become increasingly serious in the world [1]. Among a variety of pollutants, recalcitrant organic contaminants such as dyes and antibiotics are of special concern because they are difficult to degrade by means of common physical and chemical methods [2,3]. For this reason, advanced oxidation processes such as Fenton reaction have been widely applied to remediate refractory organic pollutants from water and soils [4,5].

However, classic Fenton is only effective under very acidic conditions, which inevitably cause soil acidification and massive amounts of iron sludge [6,7]. To overcome these drawbacks, heterogeneous catalysts were recently employed to replace homogeneous catalyst Fe^{2+}, and the corresponding process is called Fenton-like or modified Fenton [8]. Previous studies have shown that iron oxide nanoparticles including magnetite (Fe_3O_4) [9–11], goethite (α-FeOOH) [12], hematite (α-Fe_2O_3) [13] and maghemite (γ-Fe_2O_3) [14,15] were often used as heterogeneous Fenton-like catalysts. Furthermore, supported heterogeneous catalysts were developed to avoid the aggregation of nano-scaled catalysts [16,17], and common supports include zeolite [18,19], carbon xerogels [20], carbon nanotube [21], alginate beads [22], Nafion membrane [23], cationic exchange resin [24], and so on.

Most of current studies related to heterogeneous Fenton-like reactions have just been focused on the application of water treatment, while there is no information on the investigation of heterogeneous Fenton-like catalysts for the purpose of subsurface remediation. Although naturally existing iron minerals may catalyze H_2O_2 in some area, extremely low efficiency and complex soil heterogeneity make it necessary to supplement the extra heterogeneous catalysts in the practical application [25]. Indeed, the most desirable application of heterogeneous Fenton-like reactions for subsurface remediation is the *in-situ* injection of chemical oxidants including H_2O_2 and catalysts into the soil [26]. In this regard, mobility of catalysts in subsurface is becoming of great importance as removal efficiency is determined by the contact among organic pollutants, catalysts and H_2O_2. However, it was reported that current supports are generally larger than 2 μm, which are not movable under typical subsurface conditions according to classical filtration theory and the corresponding Tufenkji–Elimelech model [27–29]. Therefore, common supported

* Corresponding author.
E-mail address: jingjingzhan@dlut.edu.cn (J. Zhan).

https://doi.org/10.1016/j.cclet.2019.09.001

heterogeneous catalysts in micron size range are not suitable for the *in-situ* Fenton-like treatment of contaminated soil due to their inappropriate size and the resultant poor mobility in the subsurface, although they offered excellent performance for water purification.

The objective of this paper was to present a heterogeneous Fenton-like catalyst which could be applied in subsurface remediation. In this study, submicron γ-Fe_2O_3/C spheres were synthesized through a facile one-step aerosol-based process, followed by the evaluation of their transport properties, pollutants adsorption and H_2O_2-activating ability. Our results revealed that as-prepared composites may hold the following advantages for future applications: (1) the optimum size in the range of 100 nm – 1 μm guarantees that the composites effectively transport through sediments and easily reach the contamination zone, beneficial for *in-situ* subsurface remediation; (2) immobilization of γ-Fe_2O_3 into carbon spheres cause less prone to aggregation and negligible iron leaching, and thus maintaining high H_2O_2-activating ability; (3) carbon serves as a strong adsorbent in addition to a support and therefore helps to uptake the pollutants from soil, facilitating the contact of catalysts–pollutants and enhancing the removal efficiency. To the best of our knowledge, this is the first report of a heterogeneous Fenton-like catalyst with good mobility intended for use in soil and groundwater remediation,

We synthesized submicron γ-Fe_2O_3/C spheres using a self-built aerosol setup as depicted in Fig. 1. The procedure is similar to our earlier work [30–32], but a commercial nebulizer (402AI, Jiangsu Yuyue Medical Equipment & Supply Co., Ltd.) instead of the costly atomizer nozzle was firstly used, paving the way for the future scale-up. Typically, 6 g of sucrose and 5 g of $FeSO_4{\cdot}7H_2O$ were firstly dissolved in 40 mL deionized water. Then, the precursor solution was ultrasonically nebulized to droplets and pass through a heating zone driven by the carrier gas (N_2). The temperature was held at 900 °C in the heating zone. The produced black particles were collected by two consecutive water bubblers. Subsequently, the obtained particles were washed by deionized water for several times to remove purities and dried at 60 °C before use. In the process, each aerosol droplets containing sucrose and iron sulfate went through the high temperature zone, where sucrose dehydration (Eq. 1) and iron sulfate decomposition (Eq. 2) took place, resulting in the formation of γ-Fe_2O_3/C spheres.

$$C_{12}H_{22}O_{11}(\text{sucrose}) \xrightarrow{\Delta} C + H_2O \uparrow \quad (1)$$

$$FeSO_4 \xrightarrow{\Delta} Fe_2O_3 + SO_2 \uparrow + SO_3 \uparrow \quad (2)$$

The morphology and microstructure of the particles was characterized by SEM, TEM, XRD and the N_2 adsorption. The characterization method and equipment are depicted in Supporting information. As shown in Fig. 2a, the SEM image indicates the obtained materials are spherical with variable size ranging from 100 nm to 1 μm, which is the typical feature of materials synthesized through aerosol-based process [33–36]. Furthermore, the TEM image (Fig. 2b) illustrates an even distribution of iron oxides without aggregation throughout the carbon matrix. All diffraction peaks in the XRD pattern (Fig. 2c) are well matched with the correspondence planes of γ-Fe_2O_3 according to JCPDS No. 39-1346. In addition, the N_2 adsorption isotherm of γ-Fe_2O_3/C is shown in Fig. 2d, which reveals that the surface area was 231.0 m^2/g, calculated by the Brunauer–Emmet–Teller (BET) method. The pore volume was 0.364 cm^3/g based on Barret–Joyner–Halenda (BJH) model. In fact, the porosity of supports is desired in the application, which may ensure the convenient entry of H_2O_2 to contact the surface of the interior iron oxides.

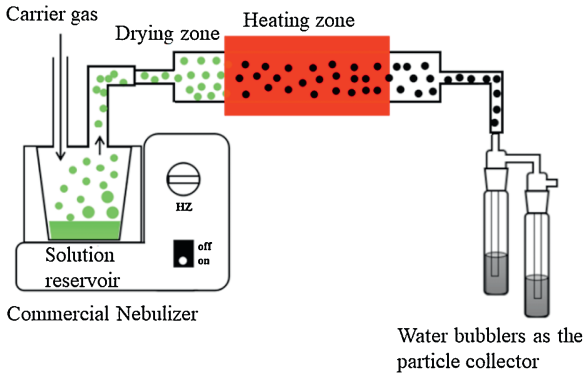

Fig. 1. Aerosol-assisted experimental apparatus.

Classic filtration theory assumes that three mechanisms including diffusion, interception and sedimentation account for the trajectory of colloidal particles through porous media such as soil. Furthermore, the Tufenkji-Elimelech equation calculated the theoretical single contact efficiency (η_0) to predict the collision probability of migrating particles with the collector. Apparently, the lower contact efficiency implies the better transportability on the premise of the same attachment efficiency. Intuitively, the smaller particles could transport more effectively through the sand. However, we have correlated the collector efficiency with particle size, where a concave curve (Fig. 3a) displays the optimal size for γ-Fe_2O_3/C and bare Fe_2O_3 particles to freely move through porous media is in the submicron scale (300 nm – 1 μm is the best) under conditions closed to most sediment systems. The details of η_0 calculation has been shown in Supporting information.

The mobility of submicron γ-Fe_2O_3/C spheres in the subsurface was evaluated by a series of sand-packed column experiments, which were designed to simulate the injection of heterogeneous catalysts into water-saturated porous media. The column tests were based on a common 50 mL glass burette. In the experiment, the column was firstly packed with dry sand, which was in the size range of 300–700 μm. During the packing, intermittent vibration was adopted to ensure uniform packing and the packed volume was maintained at 20 mL. A small cotton plug was placed at the bottom of each column to prevent the loss of the sand. Then, the column was saturated with water prior to the injection of the materials containing suspension. The porosity of the column was determined as 0.42 following the previously reported method [29] and accordingly the pore volume (PV) was 8.4 mL. After 3 PVs of bulk suspension with desired concentration (either γ-Fe_2O_3/C or bare γ-Fe_2O_3) was fed, each column was flushed with 9 PVs of water at a flow rate of 18 mL/min (superficial velocity of 20 cm/min, controlled by a peristaltic pump). Effluent samples were collected every 1 PV. Each sample was digested by adding 3 mol/L HCl solution and the total iron concentration was measured with 1, 10–phenanthroline spectrophotometric method [37].

Fig. 3b shows visual comparison between submicron γ-Fe_2O_3/C spheres and commercial available bare γ-Fe_2O_3 nanoparticles (50–1000 nm). The concentrations of the influent suspensions were both at 3 g/L. In the case of bare γ-Fe_2O_3 nanoparticles, only clear solution passed through the columns and most of the particles were trapped at the entrance end of the column. This indicates that bare γ-Fe_2O_3 nanoparticles had poor transportability because they form aggregates rapidly and thus are easily intercepted by the porous media. In contrast, submicron γ-Fe_2O_3/C spheres were able to travel through the column and elute efficiently, confirmed by the visibly black particles collected in the conical flask. Fig. 3c shows breakthrough curves of submicron γ-Fe_2O_3/C spheres with varied concentrations, which are plotted as the relative

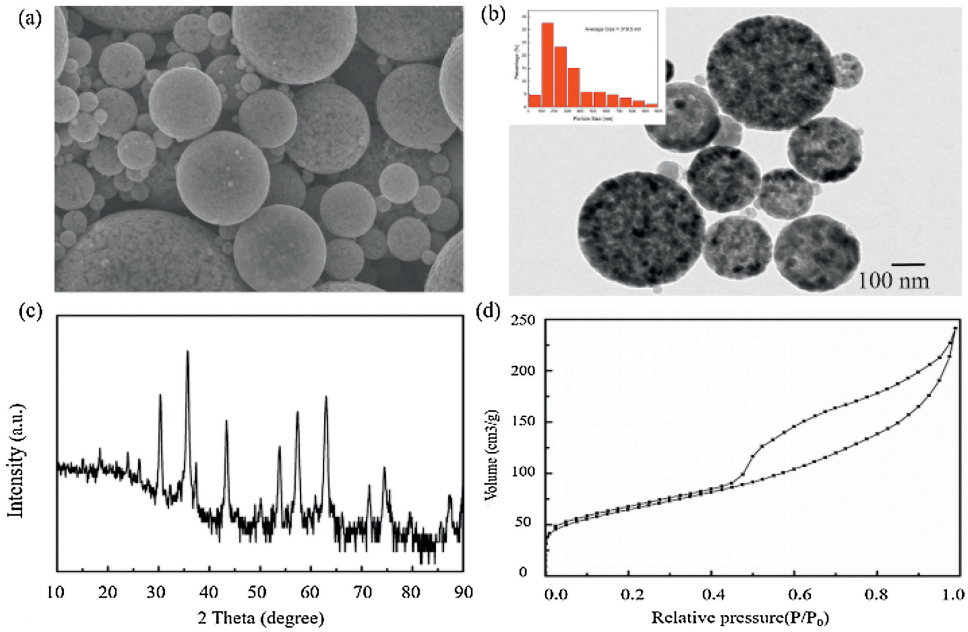

Fig. 2. (a) SEM, (b) TEM, (c) XRD and (d) Nitrogen adsorption-desorption isotherm of submicron γ-Fe_2O_3/C spheres. The inset is the size distribution of the spheres.

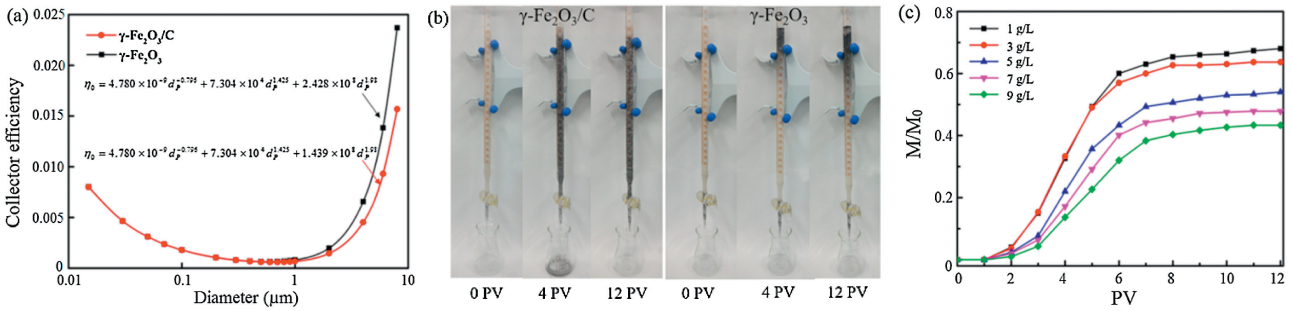

Fig. 3. (a) Collector efficiency dependency on the particle size as predicted by the Tufenkji-Elimelech filtration model. The two curves represent the theory for γ-Fe_2O_3/C and γ-Fe_2O_3. (b) Elution characteristics of submicron γ-Fe_2O_3/C spheres (left) and pristine γ-Fe_2O_3 (right); (c) Elution profiles of submicron γ-Fe_2O_3/C spheres with different initial concentrations. M/M_0: the fraction of particles that are eluted.

concentration of solid materials in the effluent (C/C_0) *versus* PVs. At 1 g/mL, almost 67.2% of particles were eluted from the sand column after flush with 12 PVs under the specified conditions. Meanwhile, the relative effluent concentration slightly decreased to 63.3% for 3 g/mL, and 42.0% for 9 g/mL.

All heterogeneous Fenton-like experiments were conducted at room temperature and the initial pH of the solution was adjusted by H_2SO_4 (0.1 mol/L) or NaOH (0.1 mol/L). In the experiment, 10 mg of submicron γ-Fe_2O_3/C spheres was firstly added into a 10 mL of methylene blue (MB)-contaminated aqueous solutions, followed by the addition of desired amount of H_2O_2. The mixture was then stirred during the reaction. At predetermined time, the experiment was terminated by the magnetic separation of γ-Fe_2O_3/C spheres from the solution. The residual MB in the supernatant was directly analyzed by an UV – vis spectrometer (5200PC, China) at wavelength of 665 nm. To determine the amount of the adsorbed MB, solid catalysts were washed by 10 mL of ethanol for three times to completely extract MB. Subsequently, the amount of degraded MB was calculated by subtracting the total of the residual and the adsorbed MB from the initial MB. In the experiments, MB was chosen as the primary probe molecule because it was a typical recalcitrant pollutant widely used in previously reported Fenton-like reactions. In addition, the remediation of sulfamethoxazole (SMX) was simply investigated as a complement, considering that it is one of frequently detected pollutants in soil and groundwater. Their structures are shown in Fig. S1 (Supporting information).

Fig. 4a shows photographs of untreated and treated MB-contaminated solutions, which visually reflect the effectiveness of the system γ-Fe_2O_3/C+H_2O_2 on the treatment of MB over a period of 4 h. A noticeable discoloration in only 10 min illustrates that most of MB has been quickly removed from the aqueous phase. However, when catalysts γ-Fe_2O_3/C spheres were magnetically separated and rinsed by ethanol, blue extractions were observed again which means that MB was initially adsorbed on the γ-Fe_2O_3/C spheres rather than oxidation. Hence, preliminary vial tests indicate that there are three possible routes for MB during the removal process including degradation due to the Fenton-like reaction, adsorption by heterogeneous catalysts and as the residual remaining in aqueous phase.

Fig. 4b presents the kinetics of MB removal and degradation in the presence of γ-Fe_2O_3/C spheres and H_2O_2, where the difference between removal and degradation is that the latter only counts the decrease of solution MB concentration arisen from Fenton-like oxidation, but the contribution from adsorption was excluded. As a control, the system combining bare γ-Fe_2O_3 nanoparticles and H_2O_2 was also studied. The removal curve of the γ-Fe_2O_3/C + H_2O_2

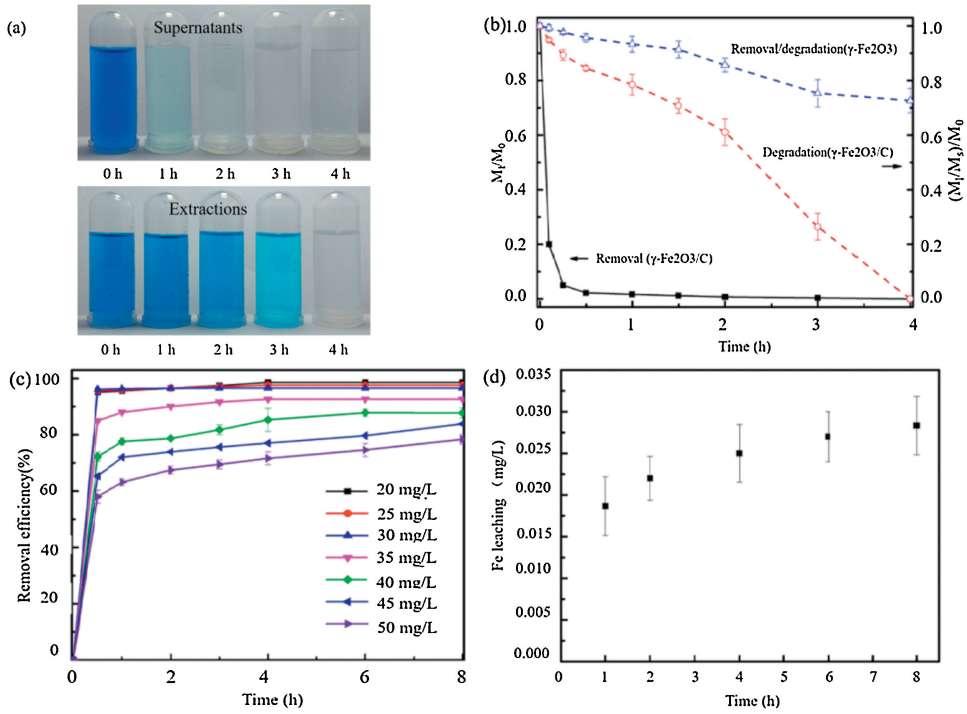

Fig. 4. (a) Photographs of supernatants and extractions of MB-contaminated solutions treated by the system γ-Fe_2O_3/C+H_2O_2 at different times. (b) MB removal and degradation rates for submicron γ-Fe_2O_3/C spheres and pristine γ-Fe_2O_3 in the presence of H_2O_2. M_l: the amount of MB remaining in the solution, M_s: the amount of MB adsorbed on the catalyst, M_0: the amount of the original MB in the solution. (c) Adsorption capacity for MB on γ-Fe_2O_3/C and (d) iron leaching during the reaction. Experimental conditions: T = 25 °C, pH 7, $[H_2O_2]_0$ = 0.2 mol/L, $[MB]_0$ = 30 mg/L, [catalyst] = 1 g/L.

system (the solid black line: M_l/M_0) exhibits an immediate sharp drop to 20.7% of its initial concentration followed by a much slower decrease. Obviously, this is mainly the result of MB partitioning from the aqueous phase to the solid surface through strong adsorption. To accurately determine the reactivity, the degradation curve of the γ-Fe_2O_3/C + H_2O_2 system (the dash red line: $(M_l+M_s)/M_0$) was presented which only counted the decrease of solution MB concentration arisen from Fenton-like oxidation, but the contribution from adsorption was excluded. From this dash line, it could been seen that 4.9%, 21.2% and 100% of MB were degraded in 5 min, 1 h and 4 h, respectively. In contrast, the removal curve and the degradation curve for the control experiment are the same because the amount of MB adsorbed on bare γ-Fe_2O_3 was negligible. Clearly, there is no pronounced decrease in MB concentration and only 28.3% of the pollutant was removed from the solution in 4 h, showing a much slower removal and degradation rate.

The adsorption ability of the γ-Fe_2O_3/C spheres was further investigated by the time-dependent adsorption capacity under different initial MB concentrations. Herein, 10 mg of γ-Fe_2O_3/C spheres and 10 mL of MB solution at 10–50 mg/L were used in the absence of H_2O_2. As shown in Fig. 4c, in each case the adsorptive capacity rises dramatically in the first few minutes, followed by the gradual increase till equilibrium.

Meanwhile, we found the adsorption fits Langmuir model where the maximum adsorption amount q_m arrives 42.166 mg/g and K_L is 2.723 L/mg. Furthermore, we compared the adsorption capability of the γ-Fe_2O_3/C spheres with the materials reported in the literature. Under the same condition with the initial concentration of MB at 40 mg/L, the uptake amounts of MB are 6.8, 6.0, and 8.0 mg/g for α-Fe_2O_3@GO, Fe_3O_4-carbon and γ-Fe_2O_3-Fe-carbon, lower than 28.8 mg/g for aerosol-assisted γ-Fe_2O_3/C spheres. In addition, similar phenomena were observed for SMX as shown in the Supporting information, where Figs. S2 and S3 (Supporting information) demonstrated removal and adsorption kinetics, respectively.

To understand whether heterogeneous γ-Fe_2O_3/C spheres or dissolved iron ions from maghemite account for the decomposition of H_2O_2, the dissolved iron concentration was measured in the experiment. As shown in Fig. 4d, the leached iron concentration was detected at ~0.028 mg/L after 6 h when 1 g/L of γ-Fe_2O_3/C spheres were used at pH 7, far below the acceptable limit of 2 mg/L according to the EU discharge standard [38]. Furthermore, the degradation efficiency at the same level of dissolved iron (~0.028 mg/L) was tested to be 4.7% in 4 h, negligible compared to the use of γ-Fe_2O_3/C spheres. Meanwhile, the supernatant obtained after 6 h was reused with the addition of H_2O_2 for another catalytic test, and no significant removal phenomenon was observed in absence of the γ-Fe_2O_3/C. Hence, it is concluded that soluble iron only existed in insufficient concentration to catalyzed hydrogen peroxide decomposition. Accordingly, the mechanism in this study is the Fe^{III}–initiated decomposition of H_2O_2 under the circumneutral conditions, involving a series of chain reactions as previously described [39].

Hence, in our understanding, the significant enhancement in the degradation rate for the γ-Fe_2O_3/C + H_2O_2 system might be attributed to two reasons. Firstly, the distribution of nano-scaled γ-Fe_2O_3 catalysts onto carbon spheres prevented the aggregation, and thus retained the number of active sites for reaction. Secondly, the strong adsorption brought about a driving force for organic pollutants from the bulk solution to the vicinity of γ-Fe_2O_3/C spheres which leads to eventual oxidization. The adsorptive-reaction system proposed here is well-suited for organic pollutants remediation in soil and groundwater as it also provides a strong sequestration from the natural organic matters such as humic acid in addition to Fenton-like oxidation.

Moreover, the effects from experimental parameters were investigated and the results are shown in Fig. 5. It is well known that pH value has a remarkable effect on the Fenton-like reaction, therefore the elimination of MB by the γ-Fe_2O_3/C + H_2O_2 system was investigated at four different pH values of 3.0, 5.0, 7.0 and 9.0.

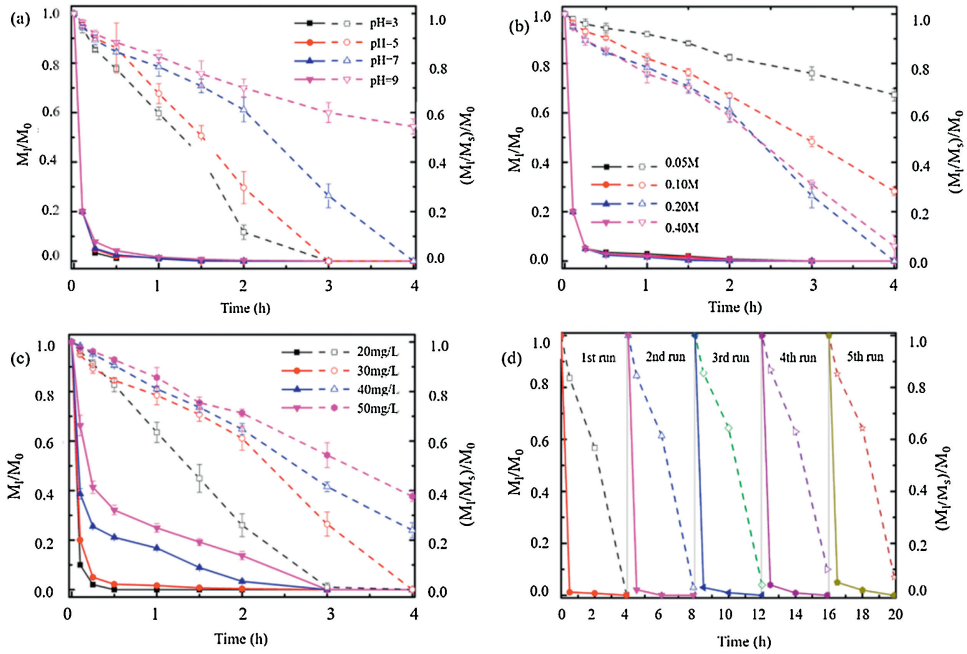

Fig. 5. Effects of (a) the initial pH, (b) the concentration of added H_2O_2 and (c) the initial concentration of MB on the removal and degradation of MB. (d) The reusability of the γ-Fe_2O_3/C. Experimental conditions (except the parameter under investigation): T = 25 °C, pH 7, $[H_2O_2]_0$ = 0.2 mol/L, $[MB]_0$ = 30 mg/L, [catalyst] = 1 g/L. Solid line is for M/M_0, and dash line is for $(M_t+M_s)/M_0$.

As seen in Fig. 5a, the MB removal efficiency was nearly unaffected by initial pH (solid lines), while the degradation efficiency decreased with an increase in the initial pH (dash lines). It should be noted that the catalytic activity of the system is enough to degrade organic pollutants at pH 7.0, and the system is still active under the alkaline condition although the degradation efficiency is lowered to 45.8% in 4 h. The wide range of the working pH is very attractive for the practical application considering the soil diversity. The higher degradation activity at the acidic condition may be related to the released Fe^{3+} ions in aqueous solution. On the contrary, the formation of $^{\bullet}OH$ on the surface of catalyst was gradually restricted with pH increasing to 9, which resulted in a slow degradation rate of MB.

The effects of the initial H_2O_2 concentration on the removal and degradation of MB were studied under the condition of $[MB]_0$ = 30 mg/L, [catalyst] = 1 g/L and pH 7. Similarly, there is no change on the removal efficiency because adsorption was not affected by the amount of H_2O_2. However, the degradation efficiency was obviously improved as the H_2O_2 concentrations increased from 0.05 mol/L to 0.2 mol/L. The reason is that the degradation efficiency is directly related to the amount of $^{\bullet}OH$ generated by the catalytic decomposition of H_2O_2, leading to much MB decomposition with the high concentration of H_2O_2. The catalyst is still active at low H_2O_2 concentration, which has a great potential for an application in soil-treatment, where a moderate amount of H_2O_2 is required for economic and technical reasons. Conversely, a slight decrease was appeared when the concentration was further increased to 0.4 mol/L (Fig. 5b). The phenomenon could be explained by the scavenging effect of $^{\bullet}OH$ by H_2O_2 according to the following equations [40]:

$$^{\bullet}OH + H_2O_2 \rightarrow {}^{\bullet}HO_2 + H_2O \quad (10)$$

$$^{\bullet}OH + {}^{\bullet}HO_2 \rightarrow H_2O + O_2 \quad (11)$$

Fig. 5c illustrates the effect that various concentration of MB had on the removal and degradation performance. With the increase of initial MB concentration from 20 mg/L to 50 mg/L, the instant drop of the removal efficiency decreased from 90.0% to 33.7% accordingly. Meanwhile, the degradation efficiency of MB in 4 h dropped from 100% to 62.3%. The reusability of the γ-Fe_2O_3/C was finally evaluated by recycling reactions for the degradation of MB under identical experimental conditions. At the end of one experiment, the material was magnetically separated from the solution and subsequently washed with ethanol and dried in a vacuum oven at 60 °C overnight before the next test. As shown in Fig. 5d, the catalyst retained a good activity after 5 cycles, despite a slight decrease in MB removal efficiency from 99% to 89% in 4 h. The result indicates that the obtained heterogeneous catalyst could still be effective when reinjection of H_2O_2 into the soil is needed.

To summary, the submicron γ-Fe_2O_3/C spheres developed in this work have exhibited the ability to be an effective heterogeneous Fenton-like catalyst for soil and groundwater remediation. Differing from the treatment of industrial wastewater, the most desirable characteristic of heterogeneous Fenton-like catalysts for subsurface remediation is to possess a good mobility in subsurface, as removal efficiency is determined by the contact among organic pollutants, catalysts and H_2O_2. The concept behind our technology involves the direct injection of γ-Fe_2O_3/C spheres and H_2O_2 into contaminated groundwater-saturated sediments. As soon as the γ-Fe_2O_3/C spheres enter into the contaminated area, the carbon component could act as an adsorbent for organic pollutants, thereby providing a driving force to capture the adsorbed contaminants from the soil to the vicinity of iron oxides for further reactions. Consequently Fenton-like reactions catalyzed by γ-Fe_2O_3 lead to eventual degradation of organic pollutants. Hence, the system containing this novel heterogeneous catalyst and H_2O_2 is able to sequester and degrade organic pollutants simultaneously in addition to move through the subsurface readily. However, we consider this work is just the first step which is necessary in determining the potential for practical applications. Several studies such as the effects of the organic matters in the soil, the competitive adsorption of cations and anions, the long term fate and transport of these materials are still in progress.

Acknowledgments

This work was supported by the National Natural Science Foundation of China (NSFC, Nos. 21876022, 31400840), the Fundamental Research Funds for the Central Universities (No. DUT16ZD226) and PetroChina Innovation Foundation (No. 2017D-5007-0609).

Appendix A. Supplementary data

Supplementary material related to this article can be found, in the online version, at doi:https://doi.org/10.1016/j.cclet.2019.09.001.

References

[1] R.P. Schwarzenbach, B.I. Escher, K. Fenner, et al., Science 313 (2006) 1072–1077.
[2] S. Rong, Y. Sun, Z. Zhao, Chin. Chem. Lett. 25 (2014) 187–192.
[3] Y. Zhang, S. Hu, H. Zhang, et al., Sci. Total Environ. 607–608 (2017) 1348–1356.
[4] B. Ranc, P. Faure, V. Croze, M.O. Simonnot, J. Hazard. Mater. 312 (2016) 280–297.
[5] J. Shi, Z. Ai, L. Zhang, Water Res. 59 (2014) 145–153.
[6] Y. Wang, H. Zhao, M. Li, J. Fan, G. Zhao, Appl. Catal. B -Environ. 147 (2014) 534–545.
[7] H. Fida, G. Zhang, S. Guo, A. Naeem, J. Colloid Interface Sci. 490 (2017) 859–868.
[8] W. Luo, L. Zhu, N. Wang, et al., Environ. Sci. Technol. 44 (2010) 1786–1791.
[9] F. Chen, S. Xie, X. Huang, X. Qiu, J. Hazard. Mater. 322 (2017) 152–162.
[10] M. Munoz, Z.M. de Pedro, J.A. Casas, J.J. Rodriguez, Appl. Catal. B -Environ. 176-177 (2015) 249–265.
[11] K. Chen, G. Wang, W. Li, et al., Chin. Chem. Lett. 25 (2014) 1455–1460.
[12] X. Qian, M. Ren, Y. Zhu, et al., Environ. Sci. Technol. 51 (2017) 3993–4000.
[13] Y. Zhao, F. Pan, H. Li, et al., J. Mater. Chem. A 1 (2013) 7242.
[14] N. Ferroudj, J. Nzimoto, A. Davidson, et al., Appl. Catal. B -Environ. 136-137 (2013) 9–18.
[15] T. Chen, Y. Xiong, Y. Qin, et al., RSC Adv. 7 (2017) 336–343.
[16] S. Zhang, X. Zhao, H. Niu, et al., J. Hazard. Mater. 167 (2009) 560–566.
[17] R.S. Ribeiro, A.M.T. Silva, J.L. Figueiredo, J.L. Faria, H.T. Gomes, Appl. Catal. B -Environ 187 (2016) 428–460.
[18] S. Navalon, M. Alvaro, H. Garcia, Appl. Catal. B -Environ. 99 (2010) 1–26.
[19] X. Yang, X. Cheng, A.A. Elzatahry, et al., Chin. Chem. Lett. 30 (2019) 324–330.
[20] R.S. Ribeiro, Z. Frontistis, D. Mantzavinos, et al., Appl. Catal. B -Environ. 199 (2016) 170–186.
[21] V. Cleveland, J. Bingham, E. Kan, Sep. Purif. Technol. 133 (2014) 388–395.
[22] O. Iglesias, J. Gómez, M. Pazos, M.Á. Sanromán, Appl. Catal. B -Environ. 144 (2014) 416–424.
[23] J. Kiwi, N. Denisov, Y. Gak, et al., Langmuir 18 (2002) 9054–9066.
[24] J. Feng, X. Hu, P. Yue, Chem. Eng. J. 100 (2004) 159–165.
[25] A.L. Pham, F.M. Doyle, D.L. Sedlak, Water Res. 46 (2012) 6454–6462.
[26] C.L. Yap, S. Gan, H.K. Ng, Chemosphere 83 (2011) 1414–1430.
[27] K. Yao, M.T. Habibian, C.R. O'Melia, Environ. Sci. Technol. 11 (1971) 1105–1112.
[28] N. Tufenkji, M. Elimelech, Environ. Sci. Technol. 38 (2004) 529–536.
[29] J. Zhan, T. Zheng, G. Piringer, et al., Environ. Sci. Technol. 42 (2008) 8871–8876.
[30] H. Qu, X. Zhang, J. Zhan, et al., ACS Sustain. Chem. Eng. 6 (2018) 7380–7389.
[31] J. He, Y. Long, Y. Wang, C. Wei, J. Zhan, ACS Appl. Mater. Interfaces 8 (2016) 16699–16707.
[32] J. Zhan, I. Kolesnichenko, B. Sunkara, et al., Environ. Sci. Technol. 45 (2011) 1949–1954.
[33] Y.F. Lu, H.Y. Fan, A. Stump, et al., Nature 398 (1999) 223–226.
[34] L. Ai, J. He, Y. Wang, C. Wei, J. Zhan, RSC Adv. 6 (2016) 56108–56115.
[35] J. Zhan, B. Sunkara, J. Tang, et al., Ind. Eng. Chem. Res. 50 (2011) 13021–13029.
[36] Y. Long, M. Li, H. Qu, et al., RSC Adv. 6 (2016) 103910–103918.
[37] T. Xu, R. Zhu, G. Zhu, et al., Appl. Catal. B -Environ. 212 (2017) 50–58.
[38] J.H. Ramirez, F.J. Maldonado-Hodar, A.F. Perez-Cadenas, et al., Appl. Catal. B -Environ. 75 (2007) 312–323.
[39] X. Hu, B. Liu, Y. Deng, et al., Appl. Catal. B-Environ 107 (2011) 274–283.
[40] X. Xue, K. Hanna, M. Abdelmoula, N. Deng, Appl. Catal. B -Environ. 89 (2009) 432–440.